

# Lattice-gas model to understand voltage profiles of $\text{LiNi}_x\text{Mn}_{2-x}\text{O}_4/\text{Li}$ electrochemical cells

Tao Zheng and J. R. Dahn

*Departments of Physics and Chemistry, Dalhousie University, Halifax, Nova Scotia, Canada B3H 3J5*

(Received 19 February 1997)

Lattice-gas models were used to study lithium intercalation in Ni-substituted spinel  $\text{LiNi}_x\text{Mn}_{2-x}\text{O}_4$  ( $0 < x \leq 0.5$ ). Both mean-field theory and Monte Carlo simulations have been used to calculate voltage profiles of  $\text{LiNi}_x\text{Mn}_{2-x}\text{O}_4/\text{Li}$  electrochemical cells. Plateaus near 4.7 and 4.1 V in the voltage profiles are believed to be related to the removal of electrons from states on the Ni  $3d e_g$  level and from the Mn  $3d e_g$  level, respectively. The structure in the voltage profiles can be qualitatively explained using nearest-neighbor repulsive interactions between Li atoms in adjacent  $8a$  sites, next-nearest-neighbor attractive interactions, and a binding energy to those sites that changes abruptly by 0.6 eV when all  $1-2x$  available sites for electrons in Mn  $3d$  levels are empty. Assuming that  $2x$  specific sites have one binding energy and the other  $1-2x$  sites have another is not successful in modeling the order-disorder transitions in the data. This implies that the either the Ni and Mn  $3d$  bands are delocalized or that a specific localized Ni or Mn  $e_g$  level can be reduced by a Li atom in any of a number of neighboring sites. [S0163-1829(97)03031-2]

## I. INTRODUCTION

Rechargeable Li-ion batteries can be made using lithium transition-metal oxides as the cathode and carbon or graphite as the anode.<sup>1,2</sup> In this technology the lithium ions are shuttled back and forth between the two intercalation electrodes as the battery is charged or discharged. Among the lithium transition-metal oxides, Ni-doped spinel  $\text{LiNi}_x\text{Mn}_{2-x}\text{O}_4$  ( $0 < x \leq 0.5$ ) has been found to be an interesting cathode material because it has a plateau in its voltage-capacity profile at one of the highest voltages versus Li (4.7 V) known.<sup>3,4</sup> These materials can be prepared by either a sol-gel method followed by a low-temperature heating<sup>3</sup> or by a solid-state reaction at high temperatures.<sup>4</sup> The capacity of the 4.7-V plateau changes linearly as a function of Ni content  $x$ . Using ultraviolet photoelectron spectroscopy (UPS), Gao *et al.*<sup>5</sup> deduced that the oxidation state of Ni is +2 in  $\text{LiNi}_x\text{Mn}_{2-x}\text{O}_4$ . These results agreed with those of Amine *et al.* who used x-ray photoelectron spectroscopy to reach the same conclusion.<sup>3</sup> Therefore the Ni-doped spinel can be written as  $\text{Li}^{+1}\text{Ni}_x^{+2}\text{Mn}_{1-2x}^{+3}\text{Mn}_{1+x}^{+4}\text{O}_4^{-2}$ .

When a Li atom intercalates in the transition-metal oxide host, it usually contributes its  $2s$  electron to the host. In the ‘‘rigid-band model,’’ this  $2s$  electron occupies the lowest empty states in the host. Conversely, when the Li atom is removed (de-intercalated) from the host, an electron from the topmost energy state is removed along with the ion. It is believed that the 4.7-V plateau of the  $\text{LiNi}_x\text{Mn}_{2-x}\text{O}_4/\text{Li}$  cell corresponds to the removal of electrons from the Ni  $3d e_g$  levels, and that the 4.1-V plateau corresponds to the removal of electrons from Mn  $3d e_g$  levels.<sup>4,5</sup>

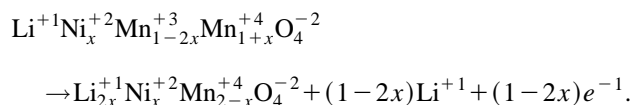
Figure 1 shows the voltage of  $\text{LiNi}_x\text{Mn}_{2-x}\text{O}_4/\text{Li}$  cells for  $x=0.1, 0.2, 0.3,$  and  $0.5$ . The voltage profile shows the two major plateaus, which can be explained using the arguments above. In addition, there are minor plateaus that are better observed if the differential capacity,  $-dy/dV$  (here,  $y$  is designated as  $y$  in  $\text{Li}_y\text{Ni}_x\text{Mn}_{2-x}\text{O}_4$ ) is plotted as in Fig. 2. Each of the major plateaus is split into two minor plateaus as

indicated by the doublets of peaks centered near 4.1 and 4.7 V. For  $x=0$ , the doublet has been explained as a result of an ordering of Li atoms at  $y=\frac{1}{2}$  onto only one of the two interpenetrating face-centered cubic (fcc) lattices that make up the  $8a$  sites on which the Li atoms reside in the spinel structure.<sup>6</sup> As  $x$  increases, it is the uppermost peak of the 4.7-V doublet that grows first. This initially surprised us. For  $x=0.2$  and  $x=0.3$ , it is the outermost peaks of the two doublets in Fig. 2 that are strongest. Only for  $x>0.3$  does the lower peak of the 4.7-V doublet grow substantially, until by  $x=0.5$ , both peaks of the 4.7-V doublet are about the same size. Our goal in this paper is to explain this behavior.

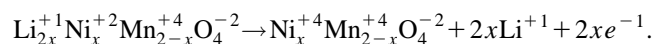
Lattice-gas models can be used to calculate the thermodynamics of intercalation compounds, where the host is a framework containing interstitial sites into which intercalant atoms can be inserted reversibly. Here, we use both mean-field theory and Monte Carlo simulations to study the voltage profile of  $\text{LiNi}_x\text{Mn}_{2-x}\text{O}_4/\text{Li}$  electrochemical cells. It is our goal to give a possible explanation for the changes that occur in Figs. 1 and 2 as  $x$  and  $y$  change.

## II. LATTICE-GAS MODEL

The 4.1-V plateau for  $\text{LiNi}_x\text{Mn}_{2-x}\text{O}_4$  can be explained as follows:



The 4.7-V plateau for  $\text{LiNi}_x\text{Mn}_{2-x}\text{O}_4$  is due to the oxidation of  $\text{Ni}^{2+}$  to  $\text{Ni}^{4+}$  shown as follows:



Therefore the capacity of the 4.7-V plateau is proportional to  $2x$  and the capacity of the 4.1-V plateau is proportional to  $(1-2x)$  as shown experimentally in Ref. 4. The total capacity over both plateaus does not change with  $x$ . Therefore, we expect a lattice-gas model of  $\text{LiNi}_x\text{Mn}_{2-x}\text{O}_4$  to have  $1-2x$

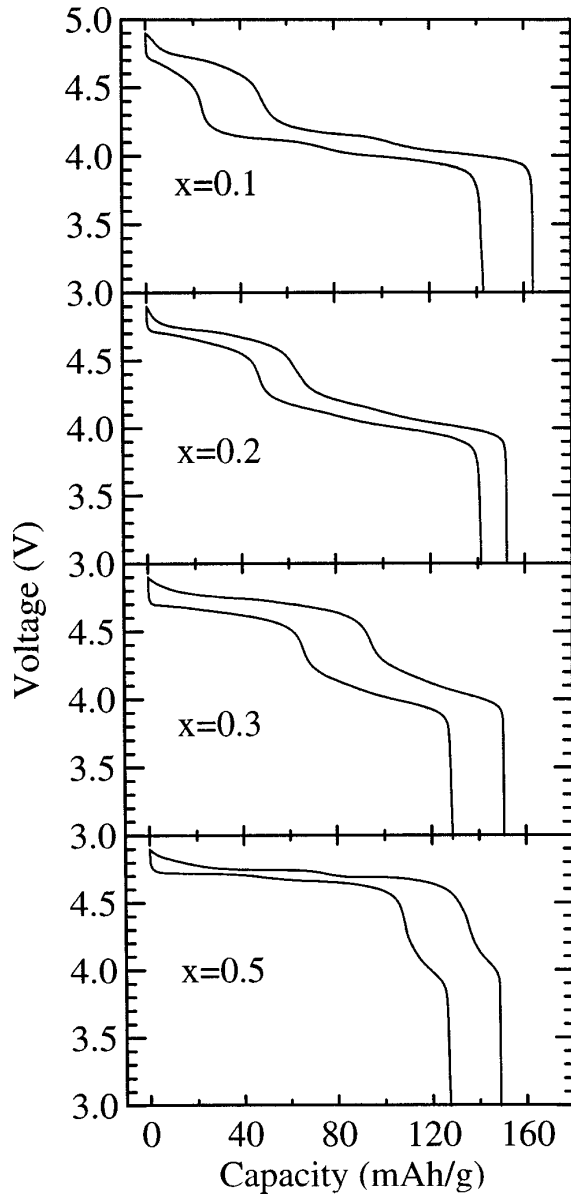


FIG. 1. The third cycles of voltage profiles for  $\text{LiNi}_x\text{Mn}_{2-x}\text{O}_4/\text{Li}$  cells with different Ni content. The value of  $x$  is shown in each panel. The data are from Ref. 3.

sites with a binding energy (with respect to Li metal) of about  $-4.1$  eV and  $2x$  sites with a binding energy of about  $-4.7$  eV.

#### A. Bragg-Williams approximation

In a lattice-gas model for the spinel structure, lithium atoms only occupy the  $8a$  sites embedded in a framework formed by Ni, Mn, and O atoms. The framework is fixed, but the  $8a$  lithium atoms are considered to be free to move during the intercalation process. The  $8a$  sites in the spinel form a diamond lattice, which can be considered as two interpenetrating fcc sublattices separated by  $(\frac{1}{4}, \frac{1}{4}, \frac{1}{4})$ . In such a lattice-gas model, we simply deal with the occupation of the  $8a$  sites. In order to treat the ordering of the Li atoms, we allow the occupation of these two sublattices to be different.

To begin, we assume that the  $2x$  sites associated with the oxidation of Ni and the  $1-2x$  sites associated with the ox-

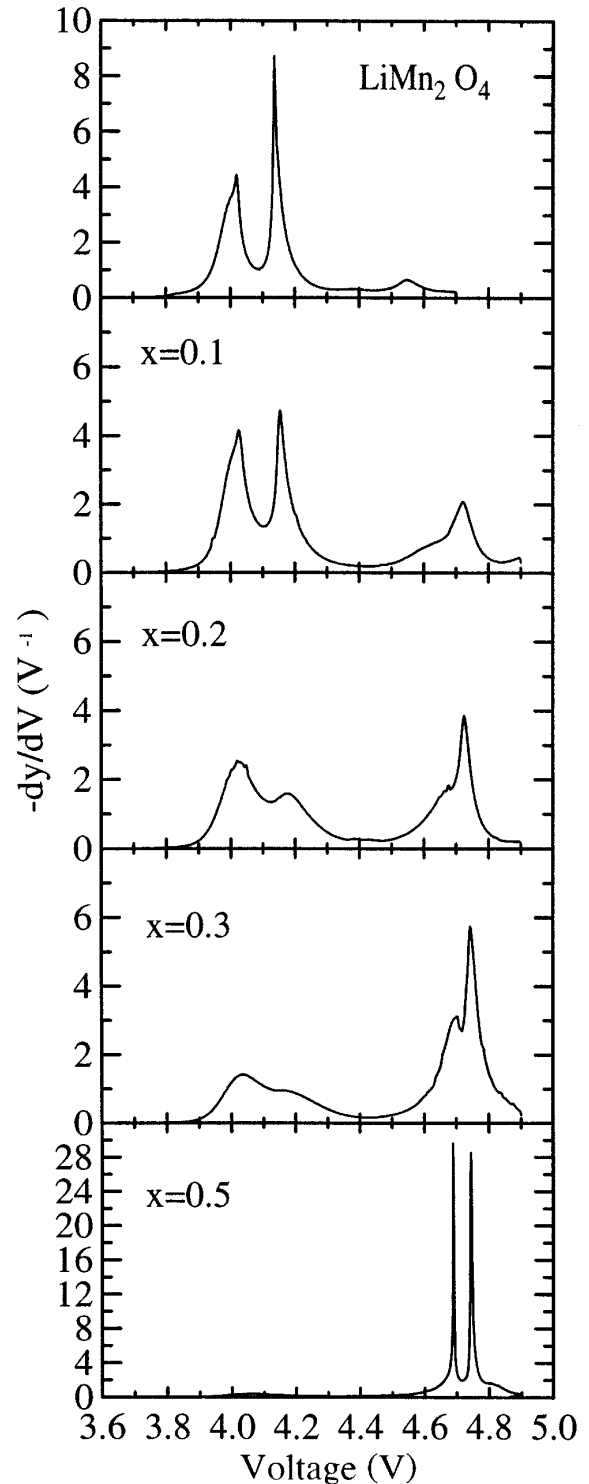


FIG. 2. Derivative curves,  $-dy/dV$  vs  $V$ , for the voltage profiles plotted in Fig. 1, where  $y$  denotes the amount of lithium per formula unit. Data for a  $\text{LiMn}_2\text{O}_4/\text{Li}$  cell are included for comparison.

idation of Mn are equally distributed over the two sublattices. This assumption is made because the Ni atoms are randomly distributed over the  $16d$  cation sites in  $\text{LiNi}_x\text{Mn}_{2-x}\text{O}_4$ . We will see below that this assumption leads to a poor description of the data. The sites associated with the oxidation of Ni are given a binding energy  $E_1$  and those associated with the

oxidation of Mn, a binding energy  $E_2$ . We expect  $E_1 \cong -4.7$  eV and  $E_2 \cong -4.1$  eV based on the data in Figs. 1 and 2.

An  $8a$  site has four nearest neighbors in the other sublattice and 12 second-nearest neighbors in the same sublattice. If we only consider the nearest- and second-nearest-neighbor interactions between lithium atoms, the Gibbs free energy of the  $8a$  lattice will be

$$G = N(E_1 y_{11} + E_1 y_{12} + E_2 y_{21} + E_2 y_{22}) + 4NJ_1(y_{11} + y_{21})(y_{12} + y_{22}) + 6NJ_2(y_{11} + y_{21})^2 + 6NJ_2(y_{12} + y_{22})^2 - T(S_{11} + S_{12} + S_{21} + S_{22}), \quad (1)$$

where  $N$  is the total number of sites on each sublattice,  $y_{ij}$  is the lithium occupation of sites of energy  $E_i$  on sublattice  $j$ , and  $J_1$  and  $J_2$  are the two-body interactions between the nearest-neighbor lithium atoms and between the second-nearest neighbors.  $T$  is the Kelvin temperature, and  $S_{ij}$  is the entropy of Li in sites on sublattice  $j$  with site energy  $E_i$ . We assume that the Li atoms in sites of energy  $E_i$  on sublattice  $j$  are randomly positioned. Therefore, the entropy  $S_{ij}$  can be obtained from

$$S_{ij} = k \ln \left( \frac{(f_i N)!}{(y_{ij} N)! [(f_i - y_{ij}) N]!} \right), \quad (2)$$

where  $f_i$  is the concentration of the sites with binding energy  $E_i$ . As discussed above,  $f_i = 2x$  for  $S_{11}$  and  $S_{12}$ , and  $f_i = 1 - 2x$  for  $S_{21}$  and  $S_{22}$ . Using Stirling's approximation,  $\ln N! \approx N \ln N - N$ , and the equilibrium of the chemical potential of Li atoms in the sites of different binding energy on the two different sublattices,  $\mu = [\partial(G/N)]/\partial y_{ij}$ , gives

$$y_{ij} = f_i \left\{ 1 + \exp \left( \frac{\epsilon_{ij}}{kT} \right) \right\}^{-1}, \quad (3)$$

where

$$\epsilon_{11} = E_1 - \mu + 4J_1(y_{12} + y_{22}) + 12J_2(y_{11} + y_{21}), \quad (3a)$$

$$\epsilon_{12} = E_1 - \mu + 4J_1(y_{11} + y_{21}) + 12J_2(y_{12} + y_{22}), \quad (3b)$$

$$\epsilon_{21} = E_2 - \mu + 4J_1(y_{12} + y_{22}) + 12J_2(y_{11} + y_{21}), \quad (3c)$$

and

$$\epsilon_{22} = E_2 - \mu + 4J_1(y_{11} + y_{21}) + 12J_2(y_{12} + y_{22}). \quad (3d)$$

Equations (3) and (3a)–(3d) can be easily solved by iteration. The amount of intercalated lithium  $y$ , is given by  $y = (y_{11} + y_{12} + y_{21} + y_{22})/2$ .  $y$  can be expressed as a function of the cell voltage  $V$ , with  $V = \mu/e$ , in order to compare to the experimental data.

Figure 3 shows calculated voltage profiles for a series samples with different  $x$ , based on Eqs. (3). The adjustable parameters were  $E_1 = -4.72$  eV,  $E_2 = -4.10$  eV,  $J_1 = 17.60$  meV, and  $J_2 = -6.06$  meV for this calculation. These parameters give a reasonable fit to the experimental result when  $x = 0.5$ . The temperature was chosen to be 30 °C as in the experiment. The repulsive interaction between lithium atoms on different sublattices and the attractive interaction between lithium atoms on the same sublattice were found to be necessary to simulate the order-disorder phase

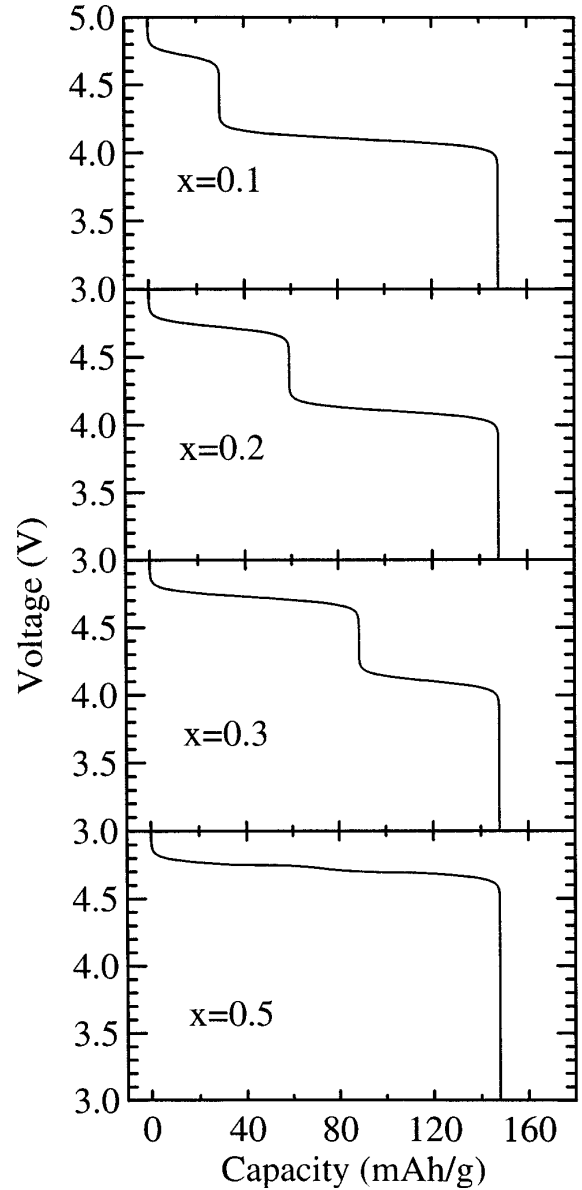


FIG. 3. Calculated voltage curves, based on mean-field theory,  $\text{Li/LiNi}_x\text{Mn}_{2-x}\text{O}_4$  cells with  $x = 0.1, 0.2, 0.3,$  and  $0.5$ , respectively.

transitions on the  $8a$  sites.<sup>6</sup> Both interactions tend to favor the ordered state, but the attractive value of  $J_2$  is needed to reduce the slope of the voltage profile and provide a match to experiment.

The calculated voltage curves in Fig. 3 show the main features of the voltage profiles observed in experiment (see Fig. 1). Figure 4 shows calculated derivative curves that correspond to the voltage profiles shown in Fig. 3. Here, the calculation does not match the experiment. Although the doublet near 4.7 V is well reproduced for  $x = 0.5$ , the peaks in  $-dy/dV$  are only broad singlets for  $x = 0.2$  and  $x = 0.3$ . The inclusion of equal numbers of sites of energy  $E_1$  on each sublattice requires that these sites fill first, in spite of the interactions. Thus, when  $x = 0.25$  and  $y = 0.5$ , each sublattice is half filled (only the sites of energy  $E_1$ ) and the order-disorder transitions are suppressed. However, when  $x = 0$  or  $x = 0.5$ , all the sites have the same binding energy and the order-disorder transitions are observed.

The flaw with the calculation can be resolved by a careful

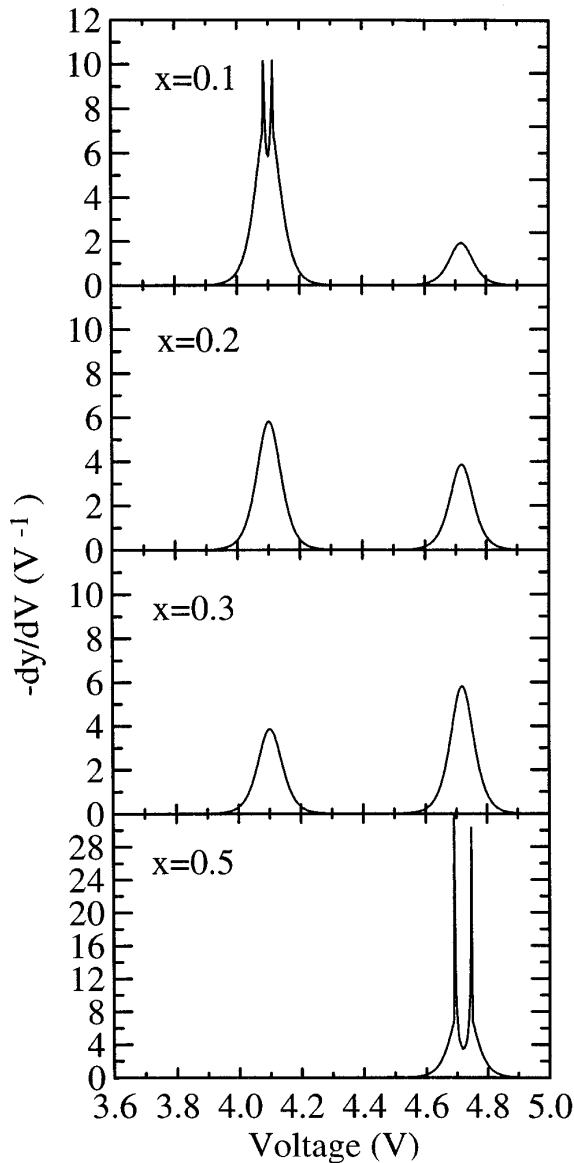


FIG. 4. Derivative curves,  $-dy/dV$  vs  $V$ , corresponding to the calculated voltage profiles shown in Fig. 3.

consideration of the data in Fig. 2, and of the physics of the intercalation in this material. Figure 2 shows that as  $x$  is increased, it is the upper peak in the 4.7-V doublet that appears first. A smooth peak in the average position of the doublet, as in the bottom panel of Fig. 4, does not appear. Consider hypothetically the deintercalation of Li for  $x=0.1$ . Initially as Li is removed, the ions can be removed from a single sublattice and the corresponding electrons are removed from Mn  $3d$  levels. At  $y=0.5$ , atoms must be removed from the second sublattice and the voltage profile steps up by an amount approximately equal to  $4J_1 - 12J_2$  to the upper plateau in the 4.1-V doublet. At  $y=0.8$ , the Mn  $3d$  levels are empty and the next electrons removed come from Ni  $3d$ , so the voltage profile steps up again by  $E_1 - E_2$  onto the upper plateau of the 4.7-V doublet. This logic can be applied schematically to the voltage profile for samples of various  $x$  as discussed next.

Figure 5 shows voltage profiles at zero temperature for several values of  $x$  and with  $E_1 - E_2 = 0.7$  eV. The order-disorder transition always occurs at  $y=0.5$ , and the voltage

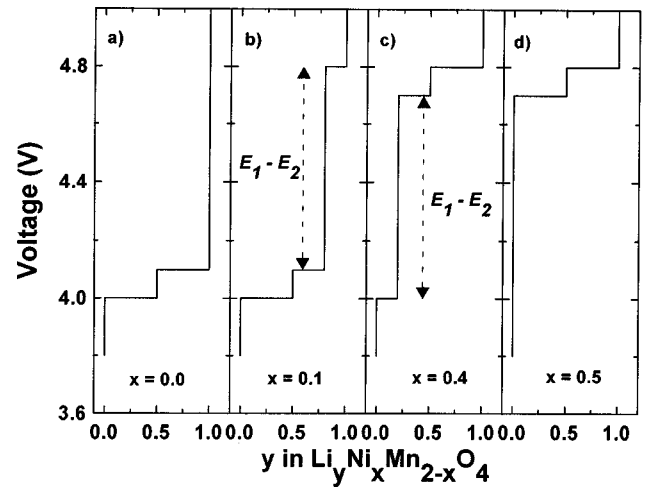


FIG. 5. Schematic zero-temperature voltage profiles as discussed in the text.

profile “steps up” by 0.7 V whenever  $y = 1 - 2x$  (because all Mn  $3d e_g$  electrons are gone). Figure 5(b) shows that in this scenario, the upper plateau of the 4.7-V doublet appears first as  $x$  increases, just as in the experiment shown in Fig. 2(b). As  $x$  increases beyond 0.25, the lower plateau of the 4.7-V doublet begins to appear as shown in Fig. 5(c).

The results in Fig. 5 qualitatively match experiment and suggest that the ordered state at  $y=0.5$  is not strongly affected by the voltage step caused by the emptying of Mn  $3d e_g$  levels. This can only occur if for  $y < 1 - 2x$  the binding energy of all the unfilled sites is  $E_2$  and for  $y > 1 - 2x$  the binding energy of all the unfilled sites is  $E_1$ . This implies that either the Ni and Mn  $3d$  levels are delocalized, or that any particular Ni or Mn atom can be reduced by a Li atom placed on a number of neighboring sites (with representation from each sublattice). We use Monte Carlo simulations to model this.

## B. Monte Carlo results

Monte Carlo simulations are used next to calculate the voltage profiles of  $\text{LiNi}_x \text{Mn}_{2-x} \text{O}_4 / \text{Li}$  cells. The calculation is performed on a lattice with a size of  $L^3 = 5 \times 5 \times 5$  conventional cells (cubic), which have the diamond structure. Periodic boundary conditions are applied. Each cubic cell with the diamond structure includes 8 sites. Therefore, the total number of available sites for lithium atoms is 1000. For each chemical potential point, the first 500 Monte Carlo simulation passes over the entire lattice are discarded so that the lattice can reach equilibrium. The next 500 passes are used for the averaging of thermodynamic quantities. In order to model the emptying of the Mn  $3d e_g$  levels at  $y = 1 - 2x$ , we abruptly change the binding energy of the sites once the average value of  $y$  reaches  $1 - 2x$ . Calculations were performed for the filling (intercalation) and the emptying (deintercalation) of the lattice so that hysteresis associated with this procedure could be studied. The hysteresis was negligible.

Figure 6 shows voltage profiles for samples with different  $x$ , calculated by the Monte Carlo method with  $L=5$ ,  $E_1 = -4.69$  eV,  $E_2 = -4.08$  eV,  $J_1 = 5.36$  meV, and  $J_2 = -1.25$  meV. These parameters give a good fit to the experi-

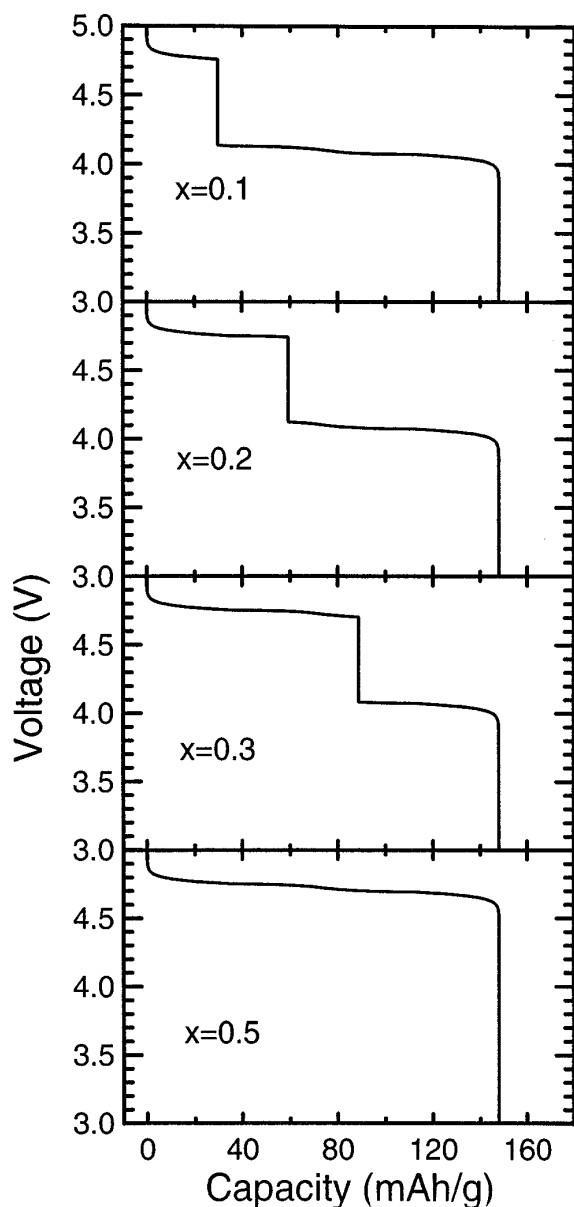


FIG. 6. Calculated voltage profiles for  $\text{Li}/\text{LiNi}_x\text{Mn}_{2-x}\text{O}_4$  cells with  $x=0.1, 0.2, 0.3,$  and  $0.5$ , respectively. The calculation is based on the Monte Carlo method assuming that the binding energy for Li changes abruptly at  $y=1-2x$ .

mental results for the case of  $x=0.5$ . The length of the 4.7-V plateau grows linearly with increasing  $x$ , while the length of the 4.1-V plateau decreases linearly so that the total capacity remains constant. When  $x=0.5$ , only the 4.7-V plateau is observed.

Figure 7 shows the derivative curves for the voltage profiles in Fig. 6. As  $x$  increases, the right-hand peak of the 4.1-V doublet shrinks and disappears, before the left-hand peak begins to reduce. Simultaneously, the right-hand peak of the 4.7-V doublet appears first and grows to a maximum, before the left-hand peak of that doublet appears. The features obtained by the Monte Carlo simulation are more or less similar to the experimental results shown in Fig. 2. However, the calculated results do not change in breadth as  $x$  changes, as the experimental peaks do. We are not sure how to explain this.

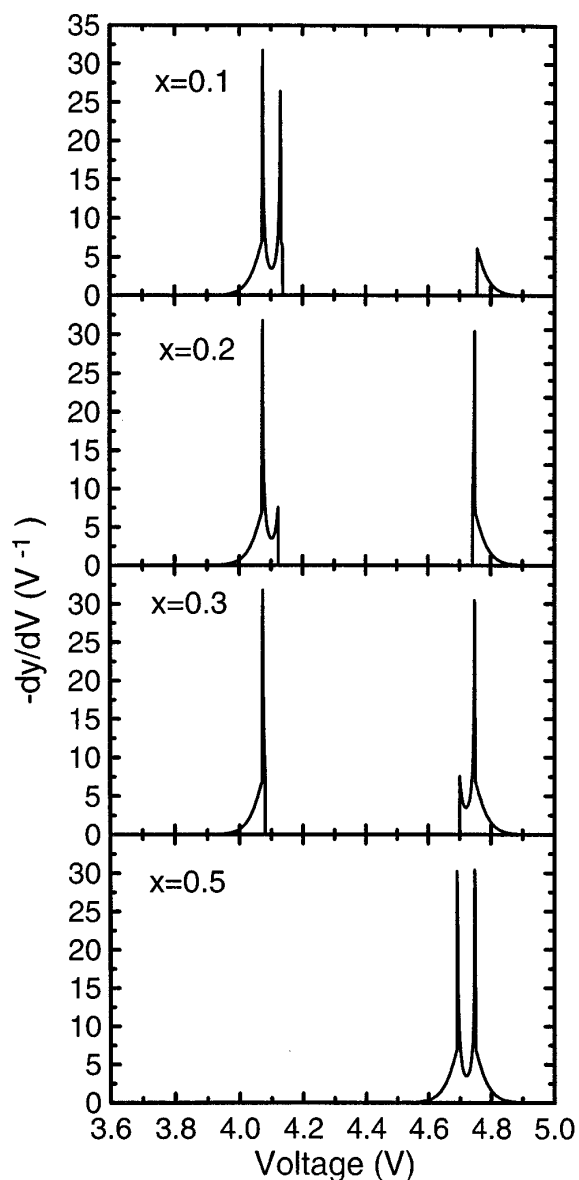


FIG. 7. Corresponding derivative curves,  $-dy/dV$  vs  $V$ , for the curves shown in Fig. 6, respectively.

### III. CONCLUSIONS

The model calculations performed here show that the changes in the voltage profile of  $\text{LiNi}_x\text{Mn}_{2-x}\text{O}_4/\text{Li}$  cells with  $x$  can be qualitatively understood if one assumes the following. (1) The ordered state at  $y=\frac{1}{2}$  persists for all values of  $x$ . One cannot associate particular binding energies with particular sites for lithium atoms. If this is done, the ordered phase is suppressed. (2) The change in binding energy at  $y=1-2x$  is of electronic origin. One should model all the sites available for Li atoms with a single binding energy, which changes abruptly at  $y=1-2x$ . Only in this way can the overall features of experiment be reproduced. This is a demonstration of the interplay between electronic and ionic effects in the intercalation solid. The Li-Li interactions are between the ions and they cause the order-disorder transition and the splitting of the 4.1- and 4.7-V plateaus into doublets. These interactions, however, cannot be considered in isolation from the changes in the electronic structure that occur with  $x$  and  $y$ , for it is these that cause the large step between the 4.1- and 4.7-V plateaus.

- <sup>1</sup>T. Nagaura and K. Tozawa, *Prog. Batteries Solar Cells* **9**, 209 (1990).
- <sup>2</sup>J. R. Dahn, U. von Sacken, M. W. Juzkow, and H. Al-Janaby, *J. Electrochem. Soc.* **138**, 2207 (1991).
- <sup>3</sup>K. Amine, H. Tukamoto, H. Yasuda, and Y. Fujita, *J. Electrochem. Soc.* **143**, 1607 (1996).
- <sup>4</sup>Q. Zhong, A. Bonakdarpour, M. Zhang, Y. Gao, and J. Dahn, *J. Electrochem. Soc.* **144**, 205 (1997).
- <sup>5</sup>Y. Gao, K. Myrtle, M. Zhang, J. N. Reimers, and J. R. Dahn, *Phys. Rev. B* **54**, 16 670 (1996).
- <sup>6</sup>Y. Gao, J. N. Reimers, and J. R. Dahn, *Phys. Rev. B* **54**, 3878 (1996).